18

Spectral response of a microresonator containing a double quantum dot modified by Coulomb interaction of localized electrons

© A.V. Tsukanov

Valiev Institute of Physics and Technology, Russian Academy of Sciences,
117218 Moscow, Russia

e-mail: a-v-ts@mail.ru

Received August 25, 2021
Revised October 15, 2021
Accepted October 22, 2021

A theoretical model of a semiconductor nanostructure consisting of a single-mode microresonator containing two quantum dots is considered. It is shown that the Coulomb interaction between electrons localized in the quantum dots modifies a spectral response of the system to an external laser field. The possibility of its use for detecting an elementary charge in the third (optically inactive) quantum dot is discussed. The influence of both diagonal (Stark effect) and non-diagonal (Foerster effect) Coulomb matrix elements of the Hamiltonian on the detection accuracy is studied. The dependences of a measuring contrast on the parameters of the resonator and the quantum dots are calculated. The existence of such structural configurations for which the contrast retains an optimal value even at large distances to the measured dot is established.

Keywords: quantum dots, microresonators, nanophotonics, semiconductors, laser, measurement

DOI: 10.21883/EOS.2022.02.53225.2678-21

Introduction

Nanostructures consisting of semiconductor quantum dots (QDs) [1] are often considered as elementary information carriers of a new generation. Arrays of single-electron QDs are proposed to be used for storing, moving and processing data in both classical and quantum computing devices [2–4]. In addition, there are diagrams of high-tech devices that are also related to practical application of QDs in modern information and communication networks [5]. These include sources of single photons [6] and correlated photon pairs [7], cellular automata [8], phase and frequency converters [9, 10], as well as sensor devices — single-electron transistors [11,12] and quantum point contacts [13]. The operating principle of capacitive sensors is based on the dependence of the energy levels position of an electron in QD which is a part of the device, and hence the quantum nanoampere current through QD from the external electric field.

The Coulomb interaction of QD electrons with each other and with external charged systems modifies the device state, therefore can serve as an additional resource for optimizing the measurement procedure. The main feature of the electron-electron interaction (unlike, e.g., electron-photon effects) is that it cannot be turned off. This must be taken into account when creating quantum registers, since the Coulomb shift of the electronic levels of a given QD qubit in the field of neighboring qubits? electrons leads to an additional phase shift of its state, which requires the use of additional corrective algorithms. Design of sensors where charged QDs are used requires the same careful approach.

In this article we consider a model of a hybrid optoelectronic system, where, in contrast to the traditional charge measurement design, we analyze the dependence not of the electric current flowing from the source to the drain directly through the QD, but of the subphoton signal passing from the laser to the photodetector through a microcavity (MC) [14]. Since photons do not interact with a charged object outside MC, it is necessary to organize an effective contact between them by supplementing the circuit with a transducer element. One can take one or several charged QDs located in the antinodes of the MC mode as such an element for exchanging an energy quantum with it and, at the same time, interacting with the object according to the Coulomb law. Thus, indirect connection is implemented between the photons going from the source to the detector through MC and the charged object [15]. Here, the role of the object is played by QD, which is located at a considerable distance from MC. In the course of a theoretical study, an analytical expression was obtained for the response of a system with two QD transducers in the subphoton mode. The effect of the Stark and Foerster components on the measurement contrast is studied within the scope of the density matrix formalism. It is shown that enhancement of the Foerster energy exchange between resonant QDs when they approach each other can help to maintain high values of the measurement contrast even for distant QDs.

Model of the optoelectronic structure and basic equations

A necessary component of many quantum-optical devices are photonic crystals (PC), which are rods or plates with lithographically made vertical holes [16]. These holes

form an ordered Bragg structure (lattice), which makes it possible to localize the photon field inside PC. The PC spectrum is divided into forbidden and allowed zones (frequency intervals with a quasi-continuous distribution of eigenmodes). In this case, lattice defects — missed holes — help to carry out further engineering of the spectral properties of PC. Extended one-dimensional defects can function as waveguides connecting the QD structure with a photon source or detector. Defects formed by just a few missed holes are microcavities with a discrete set of eigenmodes. PC-based structures are used as optical sensors for pressure, temperature, mechanical stresses, and chemical composition of samples under study [17]. However, to use them as detectors of electric fields and individual elementary charges, it is necessary to organize the interaction of photons, transported through PC, with these fields (charges). In themselves, they do not interact, therefore, for this purpose, a special circuit element — a transducer is used, which is simultaneously connected to both subsystems.

We will consider one-dimensional PC with a lattice defect (MC), which supports isolated modes with frequencies close to the frequencies of electronic transitions in semiconductor QDs (Fig. 1). If there is one QD in the high-Q MC region, the frequency of which corresponds to the frequency of the MC mode, the system is described by the well-known Jaynes-Cummings model, demonstrating Rabi oscillations (periodic transformation of the QD electronic excitation to a MC photon and vice versa). If the MC contains two or more such QDs, evolution of this system will be determined by the ratio of the characteristic energies of the electron-photon and Coulomb interactions. It is these QDs whose frequencies, on the one hand, depend on external fields and charges and, on the other hand, affect passage of photons through MC can serve as a transducer.

Let there be two QDs inside MC, each of which contains two one-electron states (ground and excited). The ground state of the $|g_k\rangle$ QD with number k ($k = 1, 2$) has energy $\varepsilon_{g,k}$, and its excited state $|e_k\rangle$ — energy $\varepsilon_{e,k}$. The laser with the frequency ω_L is focused on the PC input port. The rate Ω_L of photons arrival to the structure is determined by the degree of overlap between the fields of the PC mode and the laser. We will assume that the frequency ω_c of the MC mode and the frequencies of QD 1 and QD 2 are close enough to speak about the possibility of resonant photon exchange between them. The third QD, whose electron population is to be determined, has one (ground) state $|g_3\rangle$ with energy $\varepsilon_{g,3}$. It is assumed that the power of the potential barrier separating QDs is so high that the tunneling and exchange effects can be neglected: each electron remains localized in its own QD.

If we take the energy $\varepsilon_{g,1}$ as the origin, then the Hamiltonian of the MC and three one-electron QDs that do not interact with each other has the form (hereinafter, we assume $\hbar \equiv 1$):

$$H_0 = \omega_c a^\dagger a + \Delta_{2,1}|g_2\rangle\langle g_2| + \Delta_{3,1}|g_3\rangle\langle g_3| + \omega_1|e_1\rangle\langle e_1| + (\omega_2 + \Delta_{2,1})|e_2\rangle\langle e_2|, \quad (1)$$

where $\omega_k = \varepsilon_{e,k} - \varepsilon_{g,k}$ — electronic transition frequencies of QD, $\Delta_{2,1} = \varepsilon_{g,2} - \varepsilon_{g,1}$ and $\Delta_{3,1} = \varepsilon_{g,3} - \varepsilon_{g,1}$ — energy differences of the QD ground states. The Stark shifts of the QD levels due to the Coulomb interaction of electrons and equal to the diagonal matrix elements of the corresponding operator are taken into account using the Hamiltonian

$$H_S = V^{gg}_{1,2}|g_1g_2\rangle\langle g_1g_2| + V^{gg}_{1,3}|g_1g_3\rangle\langle g_1g_3| + V^{gg}_{2,3}|g_2g_3\rangle\langle g_2g_3| + V^{eg}_{1,2}|e_1g_2\rangle\langle e_1g_2| + V^{eg}_{1,3}|e_1g_3\rangle\langle e_1g_3| + V^{eg}_{2,1}|g_1e_2\rangle\langle g_1e_2| + V^{eg}_{2,3}|e_2g_3\rangle\langle e_2g_3|. \quad (2)$$

Off-diagonal Coulomb matrix elements describe resonant excitation quantum exchange between QD 1 and QD 2 without electron displacement (Foerster effect [18]):

$$H_F = V^F_{1,2}\left(|g_1e_2\rangle\langle g_2e_1| + |g_2e_1\rangle\langle g_1e_2|\right). \quad (3)$$

This process will be effective only if the transition frequencies in both QDs are close, i.e. when the condition of their resonance $|\omega_1 - \omega_2| \ll |V^F_{1,2}|$ is fulfilled. Matrix elements in expressions (2) and (3)

$$V^{g(e)g}_{k,m} = 2\int d\mathbf{r}_k \int d\mathbf{r}_m |\psi_{g(e),k}(\mathbf{r}_k)|^2 |\psi_{g,m}(\mathbf{r}_m)|^2/|\mathbf{r}_k - \mathbf{r}_m|$$

and

$$V^F_{1,2} = 2\int d\mathbf{r}_1 \int d\mathbf{r}_2 \psi^*_{e,1}(\mathbf{r}_1)\psi^*_{g,2}(\mathbf{r}_2)\psi_{g,1}(\mathbf{r}_1)\psi_{e,2}(\mathbf{r}_2)/|\mathbf{r}_1 - \mathbf{r}_2|$$

(hereinafter referred to as $V^F_{1,2} \equiv V_F$) are space integrals depending on the form of one-electron wave functions, on the distance between the QD centers, and on the relative orientation of QDs. Here, effective atomic units are taken as units of measurement: $1\,\text{e.a.u.} = Ry^* = m^*Ry/m_e\varepsilon^2$ for energy and $1\,\text{e.a.u.} = a^*_B = a_B m_e \varepsilon/m^*$ for length, where $Ry = 13.6\,\text{eV}$ — Rydberg energy, $a_B = 0.52 \cdot 10^{-10}\,\text{m}$ — Bohr radius, m_e — free electron mass, m^* — electron effective mass, ε — semiconductor permittivity. For gallium arsenide (GaAs: $\varepsilon = 12$ and $m^* = 0.067m_e$) we have $Ry = 6\,\text{meV}$ and $a^*_B = 10\,\text{nm}$. The processes of Jaynes–Cummings coherent electron-photon exchange between QD and the MC mode, as well as the pumping of the MC mode by laser photons, are described by the Hamiltonians

$$H_{JC} = -\Omega_1\left(|e_1\rangle\langle g_1|a + |g_1\rangle\langle e_1|a^\dagger\right) - \Omega_2\left(|e_2\rangle\langle g_2|a + |g_2\rangle\langle e_2|a^\dagger\right) \quad (4)$$

and

$$H_L = 2\Omega_L \cos(\omega_L t)(a^\dagger + a). \quad (5)$$

Equation (4) was derived using the rotating wave approximation, which assumes fulfillment of the $\omega_k \gg \Omega_k$ conditions. Thus, the Hamiltonian of our system is represented as a sum of Hamiltonians (1)–(5):

$$H = H_0 + H_S + H_F + H_{JC} + H_L. \quad (6)$$

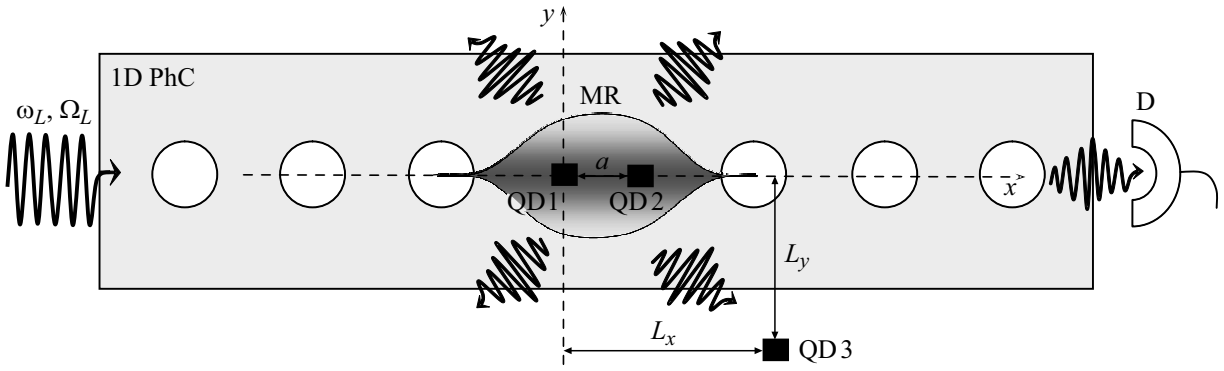

Figure 1. Diagram of one-dimensional photonic crystal with a defect (microcavity) containing two quantum dots. Their centers are located on the symmetry axis x in the antinodes of the MC mode field at a distance a from each other. The origin of the coordinates is aligned with the center of the first QD. The laser pumps the system with photons, which, passing through MC, interact with two QDs and then enter the detector or are scattered. The third (measured) QD with center coordinates (L_x, L_y), located outside MC, does not interact directly with photons, but affects the transition frequency in other (sensor) QDs due to the Coulomb interaction between them.

In addition, it is necessary to take into account noncoherent processes of photon dissipation associated with uncontrolled escape of energy from MC to the continuum at a rate κ, and electronic relaxation at rates γ_k due to the interaction of the kth QD with the phonon environment. Strict account of these phenomena is possible only within the density matrix formalism and the Lindblad equation (see below), however, an approximate solution valid for small (≤ 0.1) probability of system excitation from vacuum state can be found using a simpler (computationally) Schrodinger's equation formalism. To do this, in the expression (1) one should replace $\omega_c \to \omega_c \to i\kappa$ and $\omega_k \to \omega_k - i\gamma_k$.

If we assume that the laser pump power is low ($\Omega_L \leq \kappa$), then we can assume that no more than one excitation photon is present in the structure. Then the state space is reduced to four basis vectors. The vector $|1\rangle = |g_1, g_2, g_3\rangle|0_c\rangle$ corresponds to the vacuum state of the electron-photon system, the vectors $|2\rangle = |e_1, g_2, g_3\rangle|0_c\rangle$ and $|3\rangle = |g_1, e_2, g_3\rangle|0_c\rangle$ describe excitation of an electron in QD 1 and QD 2, and the vector $|4\rangle = |g_1, g_2, g_3\rangle|1_c\rangle$ — presence of one photon in MC mode. The system state vector $|\Psi\rangle = \sum_{k=1}^{4} c_k|k\rangle$ is represented as an expansion in basis vectors with time dependent coefficients c_k. Evolution of the state vector obeys the Schroedinger?s equation $i\partial_t|\Psi\rangle = H|\Psi\rangle$ with the initial condition $|\Psi(0)\rangle = |1\rangle$. The steady-state solution of interest to us (the average photon population of the MC) in the reference frame associated with the laser has the form

$$\langle n\rangle = |c_4|^2 \approx \frac{\Omega_L^2|\Delta_F|^2}{\begin{array}{c}|(\delta_c - i\kappa)\Delta_F - \Omega_1^2(\delta_2 - \Delta_{2,1} + G_2 - i\gamma_2),\\ -\Omega_2^2(\delta_1 + G_1 - i\gamma_1) + 2V_F\Omega_1\Omega_2|^2\end{array}},$$

$$\Delta_F = (\delta_1 + G_1 - i\gamma_1)(\delta_2 - \Delta_{2,1} + G_2 - i\gamma_2) - V_F^2, \quad (7)$$

where detunings of the MC and QD frequencies from the laser frequency are introduced: $\delta_c = \omega_c - \omega_L$ and $\delta_k = \omega_k - \omega_L$, and also the Stark shifts of the QD 1 and QD 2 frequencies are determined: $G_1 = V_{1,2}^{eg} - V_{1,2}^{gg} + V_{1,3}^{eg} - V_{1,3}^{gg}$ and $G_2 = V_{2,1}^{eg} - V_{2,1}^{gg} + V_{2,3}^{eg} - V_{2,3}^{gg}$, respectively. In the absence of interaction between QD and MC, when $|\Omega_k/\delta_k| \ll 1$, the system response coincides with the Lorentz curve for „empty" MC. If only QD 1 is optically active ($|\Omega_1/\delta_1| \gg 1$, $|\Omega_2/\delta_2| \ll 1$), and Coulomb effects can be neglected ($|V_F/\Omega_1|$, $|G_1/\Omega_1| \ll 1$), then the response curve has two polariton peaks predicted by the Jaynes–Cummings model. QD 2 involvement into resonance with the MC mode and QD 1 ($|\Omega_2/\delta_2| \gg 1$, $|G_2/\Omega_2| \ll 1$) under these conditions provides an increase in splitting of the polariton doublet by $sqrt2$ times according to the Tavis–Cummings model [15]. The spatial approach of two QDs leads to an increase in influence of Coulomb effects on the spectrum and dynamics. When the shifts G_1 and G_2 turn out to be comparable with the Rabi frequencies, the transition of the system to the dispersive regime begins. In this case, the response curve of an „empty" MC is restored, and the effect of QD is preserved in the dispersion shift $\sim (G_1^2/\Omega_1 + G_2^2/\Omega_2)$ of the peak frequency. Finally, taking into account the Foerster components under conditions of resonance of the QD transition frequencies removes their degeneration, generating a splitting of the order of $2V_F$. If the energies of the Foerster and optical interactions are approximately the same and exceed detunings and frequency shifts, hybridization of the MC photon and correlated electronic excitations in the QD group takes place. It is necessary to remember that the Stark and Foerster contributions depend on the distance between the QD centers and are, therefore, interrelated. However, QD frequency shifts due to the interaction of their electrons can be compensated by attracting an additional (independent) resource — external electrostatic field created by gates near QDs. Below, we study the effect of Coulomb contributions on the photon spectrum, focusing on the Foerster effect, and also calculate the measurement contrast by varying the distance from the structure to the measured QD.

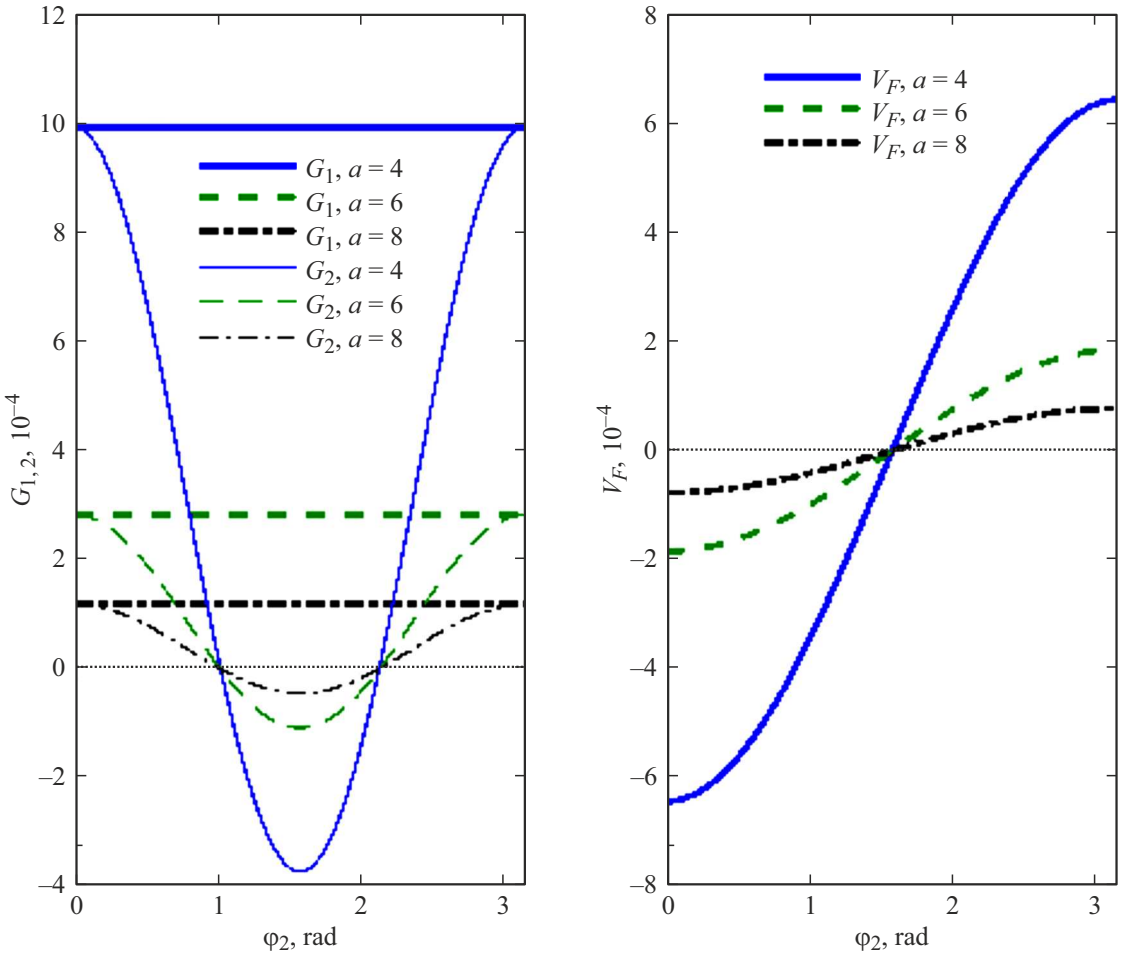

Figure 2. Graphs of dependences of the Stark (left) and Foerster (right) energies on the rotation angle φ_2 of QD 2 around the z axis, passing through its center, for three values of the distance between the centers of QD 1 and QD 2. The energies are given in units of frequency of transition to QD 1(2), and the distances — in effective atomic units.

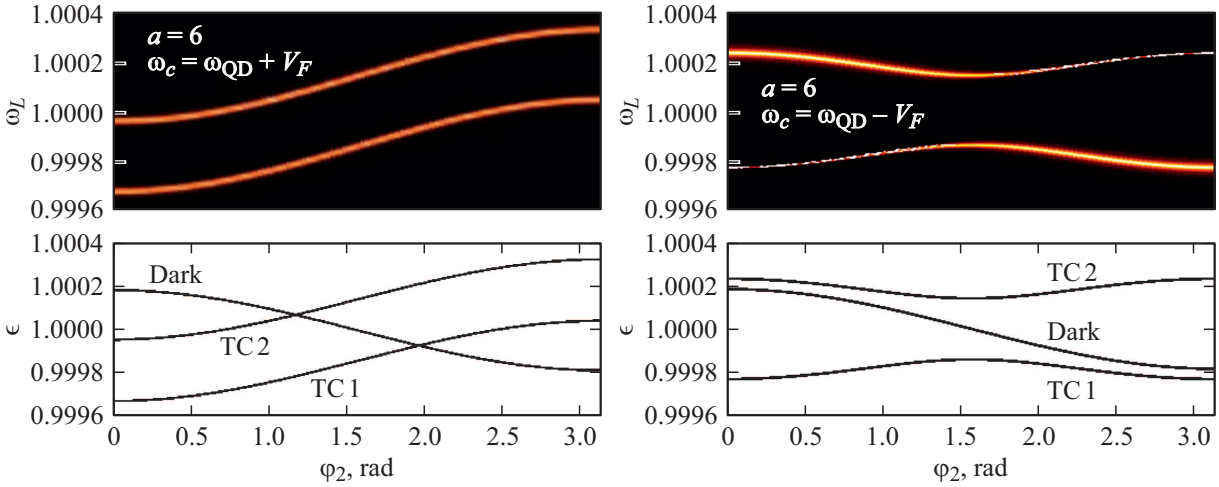

Figure 3. Graphs of dependences of the MC photon average number (upper panel) and the energies of the electron-photon Tavis–Cummings states and the „dark" state (lower panel) on the angle of rotation φ_2 of QD 2 around the axis z passing through its center. The MC frequency corresponds to the frequency of one of the Foerster doublets. All quantities are given in units of the frequency of transition to QT 1(2).

Influence of the Foerster effect on spectral response of the system

To study the spectral response of the structure, it is necessary to calculate the energies G_1, G_2 and V_F. Let us use the exponential-power approximation for the potential of the two-dimensional QD [19]:

$$U(x,y) = U_0 \exp\left[-(x/r_x)^{2p} - (y/r_y)^{2p}\right], \qquad (8)$$

where U_0 — depth of the QD potential, $2r_{x(y)}$ – length of the QD along the direction $x(y)$, and p — parameter specifying potential smoothness. At $p \geq 3$, the shape of such QD is close to rectangular. Let us select the parameters of the QD potential (8) as follows: $r_x = 0.7$, $r_y = 0.8$, $U_0 = -22$ and $p = 5$. The transition frequency $\omega_{QD} = \omega_{1(2)}$ between the ground and excited states of QD, corresponding to the MC frequency under resonance conditions, is approximately 10 e.a.u., and later on we will use this frequency as energy unit. Having found the wave functions $\psi_{g,k}(\mathbf{r})$ and $\psi_{e,k}(\mathbf{r})$ of one-electron states, we plot the dependences of the matrix elements G_1, G_2 and V_F on the distance a between the centers of two identical QDs and the rotation angle φ_2 of QD 2 relative to its center in the absence of external QD 3 (Fig. 2). The frequency shift of QD 1 G_1 remains virtually unchanged upon rotation of QD 2, which is in the ground state s, whose wave function is characterized by a weak angular dependence. The frequency shift of the rotated QD 2 is well described by the formula $G_2 \approx \frac{a_p^2}{a^3}(2-3\sin^2\varphi_2)$, obtained in the classical approximation of point charges for the effective radius of the excited p-states $a_p = 0.56$. The dependence of the Foerster energy has a feature that can not be explained using classical concepts, as in the case of Stark shifts. It can be seen from the graph that when QD 2 is rotated by an angle π and the initial charge distribution density of two QDs is restored, the Foerster energy takes on a value equal in amplitude, but opposite in sign to its initial value, $V_F(\pi) = -V_F(0)$. To obtain the initial value of this parameter, it is necessary to make a complete rotation through the angle 2π. As the distance a between QD centers increases, a rapid decrease ($\sim 1/a^3$) of all dependences is observed.

Formula (7), obtained using the Schroedinger?s equation, can be used for a qualitative analysis of the response of structures in which dephasing of the QDs' electronic state is not the predominant channel for coherence loss. In the general case, it is necessary to apply the Lindblad equation, whose solution gives the dependence of the density matrix $\rho(t)$ on time, for a given initial state $\rho(0)$:

$$\frac{d\rho}{dt} = -i[H,\rho] + \kappa D(a) + \sum_{k=1}^{2} \gamma_k D(|g_k\rangle\langle e_k|)$$

$$+ \sum_{k=1}^{2} \gamma_{d,k} D(|e_k\rangle\langle e_k\rangle - |g_k\rangle\langle g_k|), \qquad (9)$$

where $\gamma_{d,k}$ – the electron dephasing rate in the k-th QD. Dissipative photon and electronic processes are modeled by Lindblad superoperators $D(O) = O\rho O^\dagger - [O^\dagger O, \rho]/2$. According to comparison of the graphs of the dependences of the photon average number in MC on the laser frequency, obtained using approximation (7) and equation (9), the resonant frequencies coincide for both types of data. Accounting for dephasing leads to additional broadening and a decrease in the amplitude of the peaks. Thus, the analytical formula (7) gives the correct values of the natural frequencies of the system as functions of the Stark and Foerster energies.

We will consider a compact structure with a small distance between QDs and, therefore, having a noticeable Foerster exchange energy, $V_F \geq \Omega_{1,2}$. In addition, we will assume that the Stark intrastructural shifts are compensated by selecting the depths of the QD potentials. In this case, the spectrum of two one-electron QDs, provided that their frequencies are close, is a doublet with energies of the order of $\omega_{QD} \pm V_F$. Tuning the MC frequency into resonance with each of them leads to further splitting and the formation of TC1 and TC2 Tavis–Cummings doublets. The dependences of the system spectral response on the angle φ_2, as well as the eigenenergies of the Hamiltonian (1) without imaginary components and the laser field, are shown in Fig. 3 for two resonances $\omega_c = \omega_{QD} \pm V_F$. It can be seen that in addition to the optically active states with the electronic component $(|2\rangle + |3\rangle)/\sqrt{2}$, the spectrum also contains the „dark“ state $(|2\rangle - |3\rangle)/\sqrt{2}$, not excited by an external field. Increasing the distance between QD centers leads to smoothing of the angular dependence and restoration of the Tavis–Cummings spectrum. In the absence of compensation for shifts, the Hamiltonian symmetry decreases, and each of the eigenstates contains a light component. Here and below, the following set of parameters is used in calculations: $\Omega_L = 8 \cdot 10^{-6}$, $\Omega_{1(2)} = 10^{-4}$, $\kappa = 10^{-5}$, $\gamma_{1(2)} = 10^{-6}$, $\gamma_{d,1(2)} = \gamma_{1(2)}/2$ and $\Delta_{2,1} = \Delta_{3,1} = 0$.

Influence of the Foerster effect on measurement contrast

Detection of an external charge using an electron-photon structure consisting of one QD in MC is based on the difference in the values of its spectral response in the absence and presence of a charge. The external charge causes an additional Stark shift of the QD transition frequency and, as a consequence, a change in the effective energy of interaction between QD and MC. Comparing the system response $\langle n\rangle$ with the calibration dependence $\langle n_0\rangle$ obtained in the absence of an electron in the measured QD, one can determine whether the given QD contains an electron or not. The measurement is best done at laser frequency for which the difference in response is maximum. In order to quantitatively characterize the structure sensitivity to external charges and fields, we determine the measuring contrast

$$S = \max\left|\left(\langle n(\omega_L)\rangle - \langle n_0(\omega_L)\rangle\right)/\langle n_0(\omega_L)\rangle\right|. \qquad (10)$$

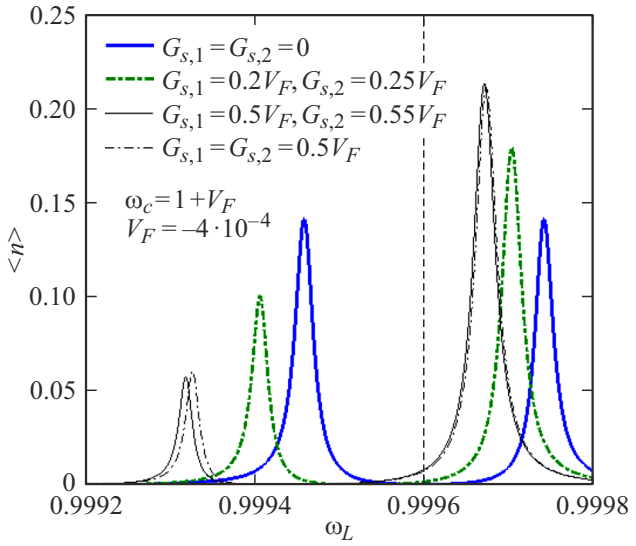

Figure 4. Spectral response of two identical single-electron QDs in MC in a steady state subphoton pumping regime with compensation for intrastructural Stark shifts. The MC frequency is tuned to resonance with the frequency of the lower hybridized two-electron state. The position of the outer QD 3 with the electron determines the frequency shifts of QD 1 and QD 2, on which the response shape depends. The vertical dashed line marks the position of the MC frequency that does not interact with the structure. All quantities are given in units of the frequency of transition to QT 1(2).

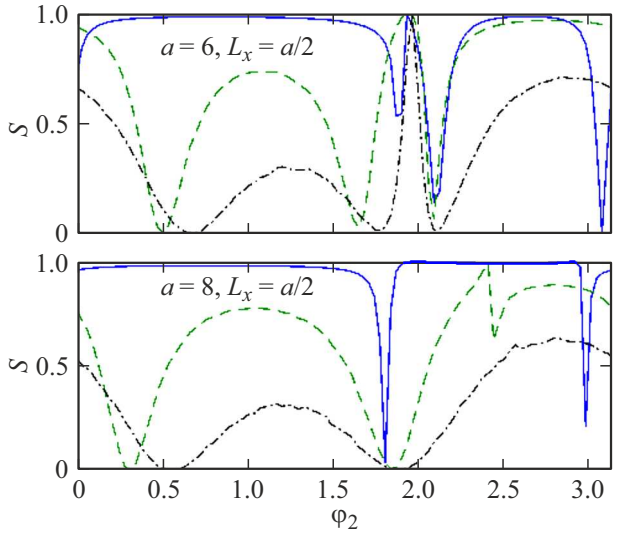

Figure 5. Graphs of dependence of contrast on QD 2 rotation angle (Foerster energy) for the distance between QD 1 and QD 2 $a = 6$ (top) and $a = 8$ (bottom). The measured QD 3 has center coordinates $L_x = a/2$ and $L_y = 4$ (solid line), $L_y = 8$ (dashed line), $L_y = 12$ (dash-and-dot line).

The value of S depends both on the properties of the QD and MC array and on the distance to the test object (in our case — to QD 3).

Addition of new resonant QDs to MC leads to an increase in splitting of the polariton peaks of the Tavis–Cummings doublet, which should increase the measurement accuracy. In this case, however, the QD frequencies are shifted due to the interaction of the QD electrons, which can significantly affect the response of the structure even in the absence of an external charge. In addition, the Foerster effect causes hybridization of the electronic states of resonant QDs due to energy exchange with each other, which also leads to frequency shifts. As was shown above, these intrastructural shifts can be partially compensated by selecting the QD parameters (dimensions, depth, orientation). If minimization of Stark shifts, which weaken connection between the electron and photon subsystems, looks justified, then the influence of the Foerster effect on the measurement accuracy requires more careful consideration. Figure 4 shows graphs of the spectral response of the structure with compensation of internal Stark shifts of QD 1 and QD 2 depending on external Stark shifts $G_{s,k} = V^{eg}_{k,3} - V^{gg}_{k,3}$ generated by an electron in QD 3. The Foerster energy $V_F = -4 \cdot 10^{-4}$ is fixed, and the MC frequency corresponds to the frequency of the lower hybridized state of QD 1 and QD 2. In the absence of an electron in the measured QD 3, the response is represented by two symmetrical Tavis–Cummings peaks shifted to the left and right of the MC frequency by $\Omega_{1(2)}\sqrt{2}$. The electron interaction, which generates small Stark shifts compared to Stark shifts $|V_F|$, causes peaks? amplitude asymmetry and shift of their frequencies. With an increase in shifts, when $G_{s,1(2)} \geq |V_F|$, „dissociation“ of the optical and electronic subsystems occurs due to violation of the resonance conditions for their frequencies. In this case, the right peak transforms to an MC peak without QD, and the amplitude of the left peak tends to zero. Under these conditions, in accordance with definition (10), the measuring contrast takes values close to unity. However, a small difference between the Stark frequency shifts of QD 1 and QD 2 (thin lines in Fig. 4) leads to a certain difference in the responses, which allows us to speak about the possibility of using the structure for differential electrometry (tracking small displacements of an external charge). Calculations show that the highest values of the difference in responses are obtained under the action of a laser with frequency corresponding to the resonant frequency of one of the peaks of the structure in the absence of an electron in QD 3.

The issue of the distance between the measured QD 3 and the structure at which the contrast S retains high values is of practical importance. Let this QD have a horizontal coordinate $L_x = a/2$ and be shifted vertically from the x axis connecting the centers of QD 1 and QD 2 by L_y. Let us set the MC frequency to be equal to the frequency $\omega_{QD} + V_F$ of the two-electron state of QD 1 and QD 2. The laser frequency is scanned in the vicinity of the lower state TC1 of the Tavis-Cummings doublet (Fig. 3) At a small distance to QD 3 ($L_y \leq a$), the shifts $G_{s,1(2)}$ are comparable with $\Omega_{1(2)}$ and $|V_F|$, which causes system transition to a nonresonant regime (solid curve in Fig. 5). In this case, the values of $S \approx 1$ are observed almost over the

entire range of the angle φ_2. (Let us recall that all the results presented in this article were obtained under the assumption that the Stark shifts are compensated by one of the methods mentioned above.) At the same time, the graphs of $S(\varphi_2)$ contain characteristic features, namely, two sharp minima, where $S \approx 0$. They narrow with increasing distance between QD 1 and QD 2, which indicates their intrastructural origin. An increase in the L_y distance reduces the effect of the charged QD 3 on the structure electron-photon spectrum, leading to the expected decrease in contrast. The function $S(\varphi_2)$ itself exhibits oscillations with an amplitude that decreases with increasing L_y. But, as follows from Fig. 5, for $a = 6$ there is a rotation angle of QD 2 $\varphi_2 \approx 2$ rad, at which the contrast retains the maximum value $S = 1$ for all three distances L_y. Since there is no similar point for a more extended structure with $a = 8$, then, taking into account the compensation of Stark shifts, this feature is uniquely associated with the Foerster effect. A similar situation is observed for the TC 2 state. As for the state of two QDs with the energy $\omega_{QD} - V_F$ and the corresponding Tavis–Cummings doublet, here the areas with a high contrast value (neighborhoods of the points $\varphi_2 = 0$ and $\varphi_2 = \pi$) are characterized by low photocurrent values, and therefore its use as a sensor state will be ineffective. At the end of our study, we point out that in the dispersive regime (without compensation for Stark shifts), the contrast decreases much faster with the distance from the structure to QD 3 [15].

The results obtained by us can be useful in development of optical sensor devices based on one-dimensional photonic crystals [20] using the principle of subphoton laser pumping in the regime of strong interaction between QD and a photon [21].

Conclusion

In this article, we consider a model of a quantum nanostructure based on a microcavity with two charged QDs with optical subphoton control, which is designed to detect individual electrons. Issues related to the influence of Coulomb effects on the measurement accuracy are studied. An approximate analytical expression is obtained for the average number of photons in the microcavity mode as a function of the control laser frequency and system parameters. The dependences of the contrast on the Foerster energy, which varies due to the rotation of one of QDs, are calculated with full compensation of intrastructural Stark shifts. It is shown that at a small distance between sensory QDs, there are configurations for which a high contrast value is retained even at a considerable distance from the structure of the measured QD. An increase in the structure size leads to the suppression of the Foerster interaction between sensory QDs, while these configurations are absent. Generally, the calculation data indicate the need to correctly take into account both diagonal and off-diagonal Coulomb matrix elements of the Hamiltonian when modeling the spectral response of such systems.

Acknowledgments

The investigation was supported by the Program No. FFNN-2022-0016 of the Ministry of Science and Higher Education of Russia for Valiev Institute of Physics and Technology of RAS.

Funding

The work was carried out within the scope of the State Order of the VALIEV IPT RAS № FFNN-2022-0016 „Fundamental and applied research in the field of development of methods for high-precision modeling and control of the element base of quantum computers“.

Conflict of interest

The author declares that he has no conflict of interest.

References

[1] B.A. Joyce, P.C. Kelires, A.G. Naumovets, D.D. Vvedensky. *Quantum Dots: Fundamentals, Applications, and Frontiers.* NATO Science Series (Springer, Dordrecht, 2003).
[2] S. Kiravittaya, M. Benyoucef, R. Zapf-Gottwick, A. Rastelli, O.G. Schmidt. Appl. Phys. Lett., **89**, 233102 (2006). DOI: 10.1063/1.2399354
[3] T. Mano, R. Nötzel, D. Zhou, G.J. Hamhuis, T.J. Eijkemans, J.H. Wolter. J. Appl. Phys., **97**, 014304 (2005). DOI: 10.1063/1.1823578
[4] T. van Lippen, R. Nötzel, G.J. Hamhuis, J.H. Wolter. J. Appl. Phys., **97**, 044301 (2005). DOI: 10.1063/1.1840098
[5] A. Walmsley. Science, **348**, 525 (2015). DOI: 10.1126/science.aab0097
[6] L. Zhang, C.-H. Teng, T.A. Hill, L.-K. Lee, P.-C. Ku, H. Deng. Appl. Phys. Lett., **103**, 192114 (2013). DOI: 10.1063/1.4830000
[7] A. Dousse, J. Suffczynski, O. Krebs, A. Beveratos, A. Lemaitre, I. Sagnes, J. Bloch, P. Voisin, P. Senellart. Appl. Phys. Lett., **97**, 081104 (2010). DOI: 10.1063/1.3475487
[8] K.K. Yadavalli, A.O. Orlov, J.P. Timler, C.S. Lent, G.L. Snider. Nanotechnology, **18**, 375401 (2007).
[9] M.P. Bakker, A.V. Barve, T. Ruytenberg, W. Löffler, L.A. Coldren, D. Bouwmeester, van M.P. Exter. Phys. Rev. B, **91**, 115319 (2015). DOI: 10.1103/PhysRevB.91.115319
[10] A.V. Tsukanov. Opt. Spectrosc., **123**, 591 (2017). DOI: 10.1134/S0030400X17100241
[11] C. Barthel, M. Kjærgaard, J. Medford, M. Stopa, C.M. Marcus, M.P. Hanson, A.C. Gossard. Phys. Rev. B, **81**, 161308(R) (2010). DOI: 10.1103/PhysRevB.81.161308
[12] DOI: 10.31857/S0544126920020088 [A.V. Tsukanov, I.Yu. Kateev. Russian Microelectronics, **49**, 77 (2020). DOI: 10.1134/S1063739720020080
[13] C.B. Simmons, M. Thalakulam, N. Shaji, L.J. Klein, H. Qin, R.H. Blick, D.E. Savage, M.G. Lagally, S.N. Coppersmith, M.A. Eriksson. Appl. Phys. Lett., **91**, 213103 (2007). DOI: 10.1063/1.2816331
[14] DOI: 10.31857/S0544126921020095 A.V. Tsukanov, I.Yu. Kateev. Russian Microelectronics, **50**, 75 (2021). DOI: 10.1134/S1063739721020098.

[15] A.V. Tsukanov. Quant. Electron., **51**, 84 (2021). DOI: 10.1070/QEL17441.
[16] R. Ohta, Y. Ota, M. Nomura, N. Kumagai, S. Ishida, S. Iwamoto, Y. Arakawa. Appl. Phys. Lett., **98**, 173104 (2011). DOI: 10.1063/1.3579535
[17] D. Yang, B. Duan, X. Liu, A. Wang, X. Li, Y. Ji. Micromachines, **11**, 72 (2020). DOI: 10.3390/mi11010072
[18] P.A. Golovinskii. Semiconductors, **48**, 760 (2014). DOI: 10.1134/S1063782614060104.
[19] M. Ciurla, J. Adamowski, B. Szafran, S. Bednarek. Physica E, **15**, 261 (2002). DOI: 10.1016/S1386-9477(02)00572-6
[20] D.-Q. Yang, X. Liu, X.-G. Li, B. Duan, A.-Q. Wang, Y.-F. Xiao. Journal of Semiconductors, **42**, 023103 (2021). DOI: 10.1088/1674-4926/42/2/023103
[21] D.A. Rasero, A.A. Portacio, P.E. Villamil, B.A. Rodríguez. Physica E, **129**, 114645 (2021). DOI: 10.1016/j.physe.2021.114645